ARMA 20–2016

A thermo-chemo-mechanical model for fault friction

Rattez, H. and Veveakis, M.
Duke university, Durham, NC, USA

This paper was prepared for presentation at the 54th US Rock Mechanics/Geomechanics Symposium held in Golden, Colorado, USA, 28 June-1 July 2020. This paper was selected for presentation at the symposium by an ARMA Technical Program Committee based on a technical and critical review of the paper by a minimum of two technical reviewers. The material, as presented, does not necessarily reflect any position of ARMA, its officers, or members.

ABSTRACT: A substantial decrease of the apparent friction has been observed in many experiments performed on synthetic or recovered fault gouges or bare rocks at seismic slip rates for different materials. This phenomenon has major implications to understand the creation of earthquakes in the brittle part of the lithosphere. These observations have become possible thank to the development of experimental machines that allow to shear the material at high velocities (up to 1m/s) under moderately high normal stresses (up to 20 MPa). In this study, we show that the weakening of the apparent friction coefficient can be explained by thermo-chemo-mechanical mechanisms. We model the fault core as an infinite sheared layer and use thermo-chemo-mechanical couplings to account for the most important processes involved in a fault zone and in the laboratory experiments. In particular, the increasing velocity during a seismic slip induces a temperature rise, which can trigger phase transformations that affect the shear stress of the system. The evolution of friction at steady state obtained from the model fits adequately results of experiments performed on various materials such as clay, halite, carbonate, granite, serpentinite and silicate.

1. INTRODUCTION

The comprehension of the apparent friction (shear strength) evolution along an existing fault zone is fundamental to characterize and understand many features of earthquakes. More specifically, the decrease of the apparent friction with increasing displacement or velocity (frictional weakening) determines the potential triggering of a seismic slip. If the frictional weakening rate is larger than a critical value determined by the release rate of elastic energy from the surrounding rock mass, this leads to the nucleation of a dynamic slip at the origin of earthquakes (Scholz 2002). In addition to nucleation, the evolution of the apparent friction coefficient determines the propagation and arrest of the fault slip and governs the form and budget of energy dissipation during seismic slip (Kanamori and Brodsky 2004). Thus, it determines the amount of energy dissipated at the fault and radiated on the surface through seismic waves and tremors, which induces catastrophic damages for infrastructures.

The development in the early 90s of the rotary shear apparatus has allowed a large set of experimental works devoted to reproducing the full range of velocities developing during a seismic slip (Ferri et al. 2011; Reches and Lockner 2010). These experiments have been performed on either fault gouges (granular samples) or bare rocks (Di Toro et al. 2011). A very large decrease of the apparent friction has been observed for velocities closed to the maximum slip velocity independently of the material considered, however the physical mechanisms accompanying this rapid weakening are different for each rock type (Rattez and Veveakis 2020). Based on and different measurements (temperature, gas emissions, etc., …) and microstructural observations on the tested samples, several thermally and mechanically activated weakening mechanisms have been suggested to understand the experimental results at different slip rates (A. Niemeijer et al. 2012). The common feature of all these weakening mechanisms is a thermally induced phase transformation (like mineral decomposition (Brantut et al. 2008; Sulem and Famin 2009; Veveakis et al. 2010), nanoparticle lubrication (Green II et al. 2015; Reches and Lockner 2010) or melting (Kim et al. 2010; Nielsen et al. 2008; A. Niemeijer et al. 2011)) during which a change in the nature of the material takes place.

In this paper, a thermo-chemo-mechanical model is developed to describe the thermal sensitivity of the mechanical behavior and the thermally induced production of weak phases during experiments performed on fault's material at different velocities. The model is able to reproduce the apparent friction at steady-state for different materials and a wide range of velocities (10^{-9} - 10 m/s). The similarity of microstructures observed in nature and in experiments suggests that energetic frameworks like the one presented here could quantitatively link observations across the scales and provide a better understanding on the physical mechanisms driving seismic slip.

2. MODEL

In this section, the thermo-chemo-mechanical model developed is briefly presented. A more detailed description can be found in (Rattez and Veveakis 2020; Segui, Rattez, and Veveakis 2019; Veveakis et al. 2010). In this model, the fault zone or the experiments performed in rotary shear, double direct shear or triaxial saw-cut configurations are represented by an infinite sheared layer (see Figure 1). In this geometry, the momentum balance equations are considered and the inertia terms are neglected (Rattez, Stefanou, and Sulem 2018):

$$\sigma_{ij,j} = 0 \tag{1}$$

where σ_{ij} is the stress tensor written following Einstein's summation convention. As we consider, a one-dimensional shear zone here, these equations lead to a constant normal and shear stress inside the layer.

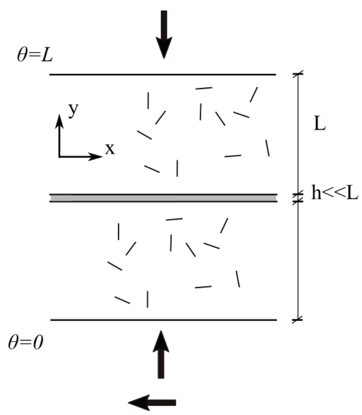

Figure 1. Geometry of the infinite sheared layer considered for the model

The constitutive law used for the mechanical behavior is a rigid elastic-visco-plastic law with the most generic form: an Arrhenius power law dependency (Frost and Ashby 1982; Veveakis et al. 2010). This constitutive relationship is only considered in a layer of thickness h, much smaller than the total thickness of the layer L (as shown in Figure 1). This enables to describe the gouge layer, which is also created in bare rocks experiments after only a few millimeters of slip. Indeed, after this small displacement, a thin layer of gouge materials forms. This layer composed of crushed grains from the initially rough surfaces has generally a thickness of 100-300 µm (Reches and Lockner 2010) and accommodates all the deformation. In the case of experiments performed on an initial gouge sample, the gouge layer presents usually a thickness of 1 mm (Rattez et al. 2018b). However, as the boundary conditions for the temperature and the weak phase are not well defined for this gouge layer, a larger domain (with a height L) is considered in order to apply Dirichlet boundary conditions for these fields. In the gouge layer, the visco-plastic constitutive relationship is:

$$\dot{\varepsilon}^{vp} = \dot{\varepsilon}^{0}\left(\frac{\tau}{\tau_y}\right)^m e^{-\frac{Q}{RT}} \tag{2}$$

where $\dot{\varepsilon}^0$ is a reference strain rate, m is the exponent of the power law, τ is the shear stress, τ_y is the yield stress, Q is an activation enthalpy for the microscopic mechanism inducing a nonlinear behavior, R is the perfect gas constant and T is the temperature. This law allows to include more physics into the hardening evolution as in the theory of plasticity for metals (Frost and Ashby 1982). The Arrhenius dependency of the flow law enables to introduce multi-physical couplings such as the effect of heat generation on the frictional strength or more generally interface phenomena between the solid skeleton and the pores (Einav 2012; Guevel, Rattez, and Veveakis 2019; Veveakis and Regenauer-Lieb 2015).

Following (Nova, Castellanza, and Tamagnini 2003), the effect of the non-mechanical state variables on the mechanical behavior of the system is expressed as a single scalar function called the weathering index $\mathrm{X_d}$. The mechanical strength of the material depends on both the plastic strain and this weathering index. It is assumed that the two dependency are uncoupled (Ciantia and Hueckel 2013) and a multiplicative decomposition of the yield stress is assumed:

$$\tau_y = T_y(\dot{\varepsilon}^{vp})\, T_y(\mathrm{X_d}) \tag{3}$$

In this study, we do not consider any purely mechanical hardening law, so that the function $T_y(\dot{\varepsilon}^{vp})$ is constant. Moreover, $T_y(\mathrm{X_d})$ is considered to be dependent on the weak phase volume fraction. For a material consisting of two species: a weak and a strong phase, occupying volumes V_w and V_s respectively, we may define the volume ratio $w = \frac{V_w}{V_w + V_s}$.

In order to constrain the form of the function $T_y(\mathrm{X_d})$, we have looked at shearing experiments performed at low velocities, in which the initial material is composed of a mixture (with different ratio) of a strong and a weak phase (Giorgetti, Carpenter, and Collettini 2015; Moore and Lockner 2011; A. R. Niemeijer and Spiers 2005; Oohashi et al. 2015; Tembe, Lockner, and Wong 2010). The results for different materials as the strong phase and two types of weak phases are shown in Figure 2. The presence of a weak phase induces decrease of the residual frictional strength along with the weak phase fraction, which is well described by an exponential law. Assuming negligible shear strength for the weak phase, this exponential evolution for $T_y(\mathrm{X_d})$ ($\mathrm{X_d}$ is assumed to be the weak phase fraction) is considered in the model and the final form of the constitutive law is therefore:

$$\dot{\varepsilon}^{vp} = \dot{\varepsilon}^0 (\frac{\tau}{\tau_0})^m e^{-\frac{Q}{RT}} e^{m\,\alpha\,w} \quad (4)$$

where τ_0 is the yield strength of the strong phase and α is the weak phase sensitivity coefficient (see (Rattez and Veveakis 2020) for a more detailed derivation).

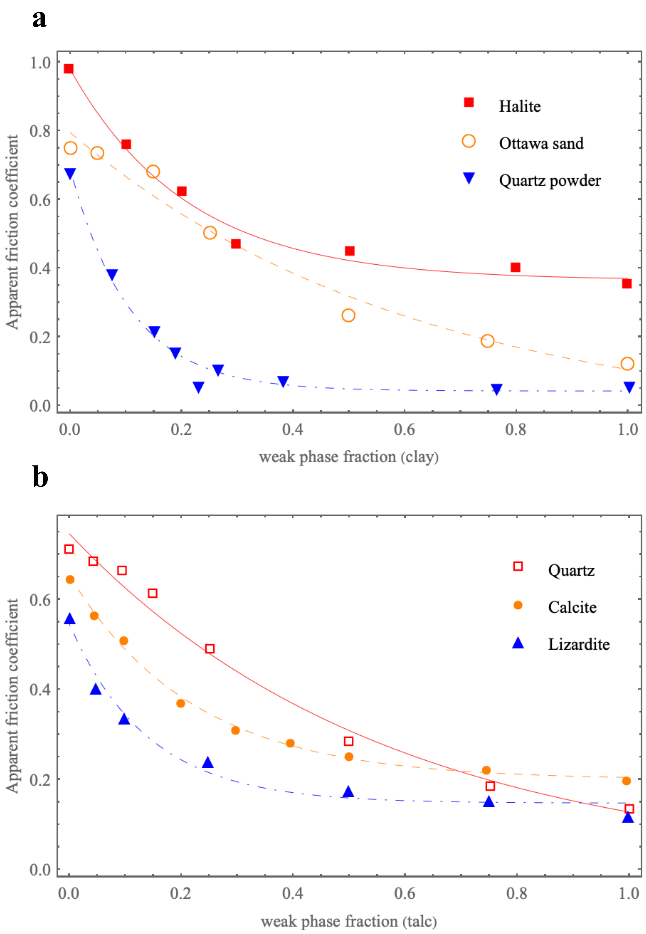

Figure 2. Effect of a weak phase fraction on the residual apparent friction coefficient for experiments performed in isothermal conditions (low velocity) with: (a) saturated clay, (b) talc, as a weak phase. The points represents the experimental data and the lines, the fitting using an exponential law. In the legend, the mineral used as the strong phase is reported.

On top of the mechanical equations, we consider the energy and mass balance equations to describe the evolution of the temperature and the weak phase fraction inside the layer:

$$\frac{\partial T}{\partial t} = c_{th}\frac{\partial^2 T}{\partial y^2} + F(y)\frac{\tau\,\dot{\varepsilon}^{vp}}{\rho C} - \frac{\Delta H\, r_F}{\rho C} \quad (5)$$

$$\frac{\partial \rho_1}{\partial t} + c_{th}\frac{\partial J_w}{\partial y} = r_F \quad (6)$$

where T is the temperature, c_{th} the thermal diffusivity, ρC the heat capacity of the mixture considered constant here, J_w the diffusion flux of the weak phase, ΔH the enthalpy of the phase change reaction considered endothermic, r_F the reaction rate and $\rho_1 = \rho_w w$. F(y) is a function which value is 1 for $y \in [-h/2, h/2]$ and 0 otherwise. The reaction rate is expressed as first order chemical reaction with an Arrhenius law:

$$r_F = (1-w)\frac{\rho_s}{M_s} k_F e^{-\frac{Q_c}{RT}} \quad (7)$$

where ρ_s and M_s are the density and molar mass of the strong phase. k_F and Q_c are the preexponential factor and activation energy of the chemical reaction respectively.

This system can be reduced to a system of two partial differential equations (Rattez and Veveakis 2020) written in a dimensionless form for the purpose of reducing the number of parameters to study and to determine the steady-states of the system (neglecting therefore the partial derivatives in time):

$$\frac{\partial^2\theta}{\partial \bar{y}^2} + F(\bar{y})Gr\, e^{\frac{Ar\,\theta}{1+\theta}} e^{\alpha\, m\, w} - Da(1-w)e^{\frac{Arc\,\theta}{1+\theta}} = 0 \quad (8)$$

$$\frac{\partial^2 w}{\partial \bar{y}^2} + \mu\, Da\,(1-w)e^{\frac{Arc\,\theta}{1+\theta}} = 0 \quad (9)$$

where, θ is the dimensionless temperature. Gr, Da, Ar and Arc are called the Gruntfest, Damköhler, Arrhenius and chemical Arrhenius numbers respectively. These numbers are defined by:

$$Ar = \frac{Q}{R\,T_0} \qquad Arc = \frac{Qc}{R\,T_0} \quad (10)$$

$$Gr = \frac{\tau_0\,\dot{\epsilon}_0\,L^2}{\rho C\, c_{th}\, T_0}\left(\frac{\tau}{\tau_0}\right)^{m+1} e^{-Ar} \quad (11)$$

$$Da = \frac{\Delta H\, k_F\, \rho_s\, L^2}{\rho C\, M_s\, c_{th}\, T_0} e^{-Arc} \quad (12)$$

$$\mu = \frac{\rho C\, c_{th}\, T_0\, M_w}{\Delta H\, \rho_w\, c_w} \quad (13)$$

The system of equations (8)-(9) is then simulated numerically using pseudo-spectral methods combined with a pseudo-arclength algorithm in order to capture all the possible steady-states for a given value of the Gruntfest number.

3. RESULTS

3.1. *Steady state of the system*

From the pseudo-arclength algorithm, we can determine the steady state of the system in the diagram of the maximum temperature as a function of the Gruntfest number (as shown in Figure 3 for a given value of the dimensionless numbers, except Gr).

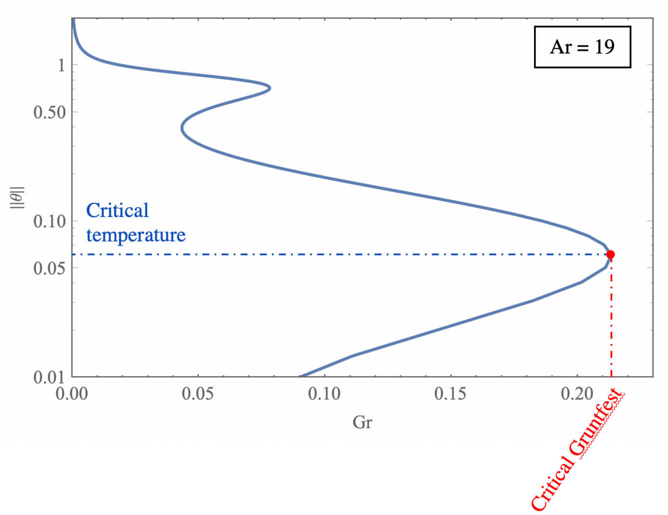

Figure 3. Maximum dimensionless temperature as a function of the Gruntfest number showing the steady state of the system of equations for a given value of the other dimensionless numbers.

If the strain rate in a rock or a granular material is high enough, the temperature increase is the main factor affecting the mechanical behavior of the material (Rice 2006) through processes like flash heating (Proctor et al. 2014) or thermal pressurization (Rattez et al. 2018a). A critical mechanical work input is necessary for these mechanisms to prevail that can be described by a critical value of the Gruntfest number, as this number expresses the ratio of a characteristic time scale of heat production over a characteristic time scale of temperature diffusion. We can therefore determine the critical Gruntfest number under which no thermal weakening is occurring. We consider here that for low velocities experiments (low Gruntfest number), the strength of the material is determined by the static friction of the materials in contact or the internal static friction of the granular assembly. For velocities larger than the critical one, the shear stress of the system is calculated by solving the thermo-chemo-mechanical model described above inside the deforming zone. The critical velocity is retrieved as a result from this model. An example is shown in Figure 3.

From this diagram of the steady state of temperature as a function of the Gruntfest number, we can calculate the corresponding diagram for the shear stress as a function of the velocity. From equations (8)-(9), the apparent friction of the layer is determined by:

$$\mu = \frac{\tau}{\sigma} = \frac{\tau_0}{\sigma}\left(\frac{c_{th}\,T_0}{\tau_0\,\dot{\epsilon_0}\,L^2}\,e^{Ar}\right)^{\frac{1}{1+m}}\,Gr^{\frac{1}{1+m}} \tag{10}$$

where σ is the normal stress applied to the layer. The velocity is calculated by:

$$v = \dot{\epsilon_0}\,L\left(\frac{c_{th}\,T_0}{\tau_0\,\dot{\epsilon_0}\,L^2}\,e^{Ar}\right)^{\frac{m}{1+m}}\,Gr^{\frac{m}{1+m}}\,e^{-\frac{Ar}{1+\theta}}\,e^{-\alpha\,w} \tag{11}$$

The resulting steady state response of the model, in terms of friction and velocity, is depicted in Figure 4. We can identify five distinct regimes of the system response to loading velocity:

(I) At low velocities, the material remains at static friction. Negligible temperature increase or weak phase production is observed.

(II) The temperature increase leads the friction coefficient to drop, in the absence of any weak phase production.

(III) With increasing velocity and temperature, small fractions of the weak phase are produced, absorbing the excess temperature and reducing the thermal softening effect on the friction coefficient. Depending on the value of the weakening coefficient, the friction coefficient can experience an intermediate increase.

(IV) Eventually, weak phase content will be produced until it reaches a critical value that will dominate the friction coefficient and lead the material to unconstrained weakening.

(V) Once the reactants are depleted (w=1), the temperature is increasing uncontrollably as the endothermic chemical reaction is not acting as a sink in the energy balance equation anymore, and the friction coefficient drops towards zero.

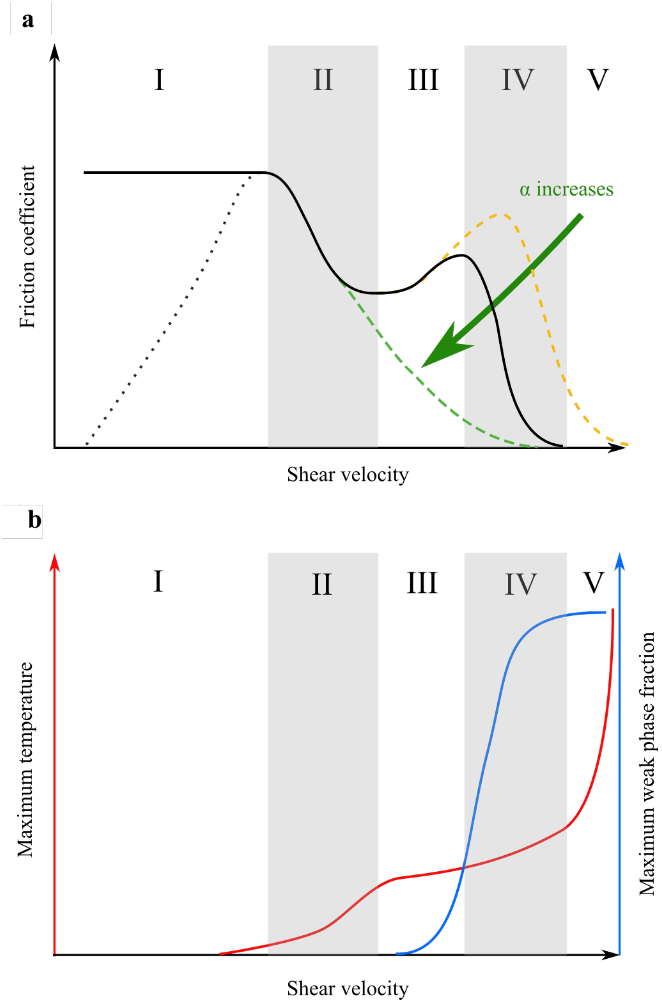

Figure 4. ***a)*** *Steady state friction coefficient as a function of velocity, for varying weak phase sensitivity coefficient α.* ***b)*** *Steady-state temperature and weak phase content dependency on the velocity.*

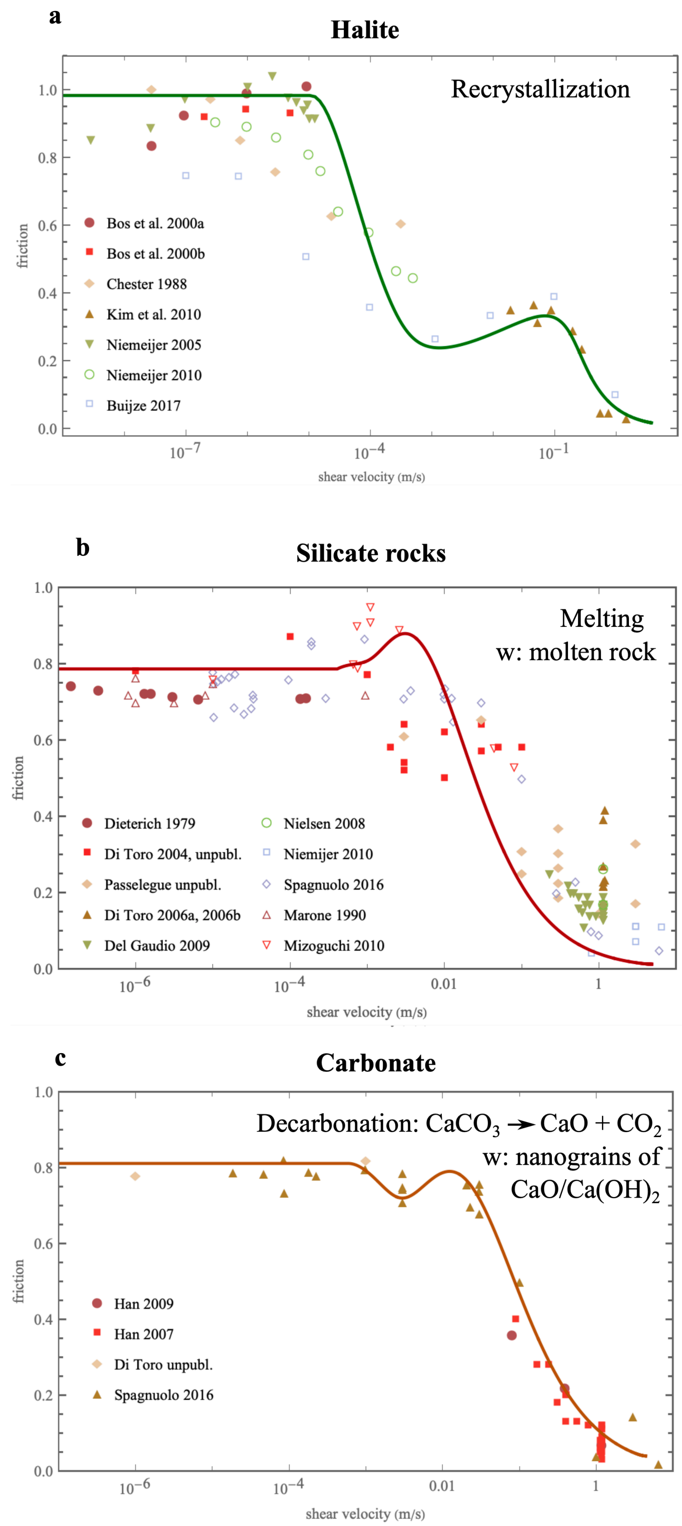

3.2. Application to different materials

After identifying the different phases of the steady frictional response of the thermo-chemo-mechanical model, it is applied to experimental data retrieved from the literature. The results are shown in Figure 5 for the steady state friction coefficient as a function of the velocity for six sets of materials (Hirose and Bystricky 2007; Spagnuolo et al. 2016; Di Toro et al. 2011). The experimental data are a collection of several independent studies at different experimental conditions. One of the interesting features of the model is the reproduction of strengthening observed experimentally at intermediate velocities (regime III in Figure 4) without supposing any additional hardening mechanism.

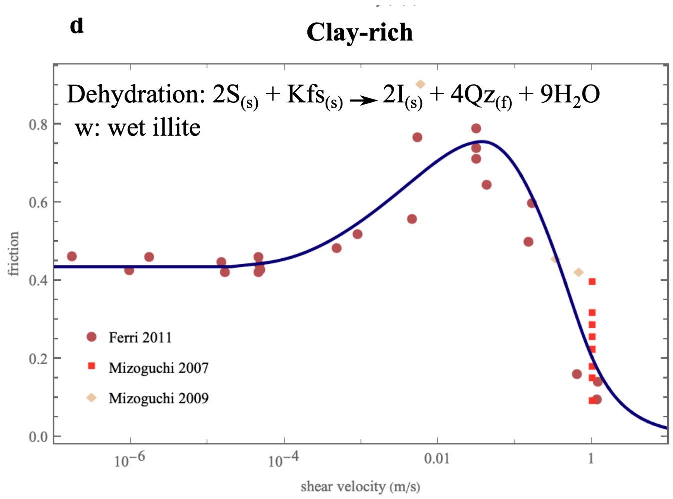

Figure 5. Application of the thermo-chemo-mechanical model (solid lines) to literature data (dots) of the friction coefficient as a function of the velocity, for a) halite, b) silicate rocks, c) carbonates and d) clay-rich materials. In each case, the phase transformation and the associated weak phase are indicated.

For each material, the model enables to capture accurately the observations and uses as input the material parameters described in (Rattez and Veveakis 2020). Moreover, it enables us to retrieve information for the parameters of the different processes such as the activation energies, together with an assessment of the temperature evolution.

4. CONCLUSIONS

In this paper, a thermo-chemo-mechanical has been developed and the steady state of the system has been determined numerically. This model has been applied to understand experiments performed on faults and enables to fit accurately the evolution of the apparent friction for the full range of velocity encountered during an earthquake. It enables to obtain valuable information about the processes affecting the mechanical behavior during these experiments and open the way to an upscaling of a physics-based model to real faults.

ACKNOWLEDGEMENTS

This work was supported by the Southern California Earthquake Center (SCEC), award number 118062196. SCEC is funded by NSF Cooperative Agreement EAR-1033462 and USGS Cooperative Agreement G12AC20038.

REFERENCES

Brantut, Nicholas et al. 2008. "High-Velocity Frictional Properties of a Clay-Bearing Fault Gouge and Implications for Earthquake Mechanics." *Journal of Geophysical Research: Solid Earth* 113(10): 1–18.

Ciantia, M O, and T Hueckel. 2013. "Weathering of Submerged Stressed Calcarenites: Chemo-Mechanical Coupling Mechanisms." *Géotechnique* 63(9): 768–85.

Einav, Itai. 2012. "The Unification of Hypo-Plastic and Elasto-Plastic Theories." *International Journal of Solids and Structures*.

Ferri, Fabio et al. 2011. "Low- to High-Velocity Frictional Properties of the Clay-Rich Gouges from the Slipping Zone of the 1963 Vaiont Slide, Northern Italy." *Journal of Geophysical Research: Solid Earth* 116(9): 1–17.

Frost, Harold J, and Michael F Ashby. 1982. *Deformation-Mechanism Maps, The Plasticity and Creep of Metals and Ceramics*. Pergamon Press.

Giorgetti, C., B. M. Carpenter, and C. Collettini. 2015. "Frictional Behavior of Talc-Calcite Mixtures." *Journal of Geophysical Research: Solid Earth* 120(9): 6614–33.

Green II, H. W. et al. 2015. "Phase Transformation and Nanometric Flow Cause Extreme Weakening during Fault Slip." *Nature Geoscience* 8(6): 484–89.

Guevel, Alexandre, Hadrien Rattez, and Manolis Veveakis. 2019. "Contact Phase-Field Modeling for Chemo-Mechanical Degradation Processes. Part II: Numerical Applications with Focus on Pressure Solution." *Preprint arXiv*.

Hirose, Takehiro, and Misha Bystricky. 2007. "Extreme Dynamic Weakening of Faults during Dehydration by Coseismic Shear Heating." *Geophysical Research Letters* 34(14): 10–14.

Kanamori, Hiroo, and Emily E Brodsky. 2004. "The Physics of Earthquakes." *Reports on Progress in Physics* 67(8): 1429–96.

Kim, Jong Wook, Jin Han Ree, Raehee Han, and Toshihiko Shimamoto. 2010. "Experimental Evidence for the Simultaneous Formation of Pseudotachylyte and Mylonite in the Brittle Regime." *Geology* 38(12): 1143–46.

Moore, Diane E., and David A. Lockner. 2011. "Frictional Strengths of Talc-Serpentine and Talc-Quartz Mixtures." *Journal of Geophysical Research: Solid Earth* 116(1): 1–17.

Nielsen, S., G. Di Toro, T. Hirose, and T. Shimamoto. 2008. "Frictional Melt and Seismic Slip." *Journal of Geophysical Research: Solid Earth* 113(1): 1–20.

Niemeijer, André et al. 2012. "Inferring Earthquake Physics and Chemistry Using an Integrated Field and Laboratory Approach." *Journal of Structural Geology* 39: 2–36.

Niemeijer, André R., and Christopher J. Spiers. 2005. "Influence of Phyllosilicates on Fault Strength in the Brittle-Ductile Transition: Insights from Rock Analogue Experiments." *Geological Society, London, Special Publications* 245(1): 303–27. http://books.google.com/books?hl=en&lr=&id=1oMGwL8ExU0C&oi=fnd&pg=PA303&dq=INFLUENCE+OF+PHYLLOSILICATES+ON+FAULT+STRENGTH+IN+THE+BRITTLE-

DUCTILE+TRANSITION+:+INSIGHTS+FROM+ROCK+ANALOGUE&ots=zNuiNFiysE&sig=zxHMgPGXol-XR5subsZ5Crtn5gA.

Niemeijer, André, Giulio Di Toro, Stefan Nielsen, and Fabio Di Felice. 2011. "Frictional Melting of Gabbro under Extreme Experimental Conditions of Normal Stress, Acceleration, and Sliding Velocity." *Journal of Geophysical Research: Solid Earth* 116(7): 1–18.

Nova, Roberto, R. Castellanza, and C. Tamagnini. 2003. "A Constitutive Model for Bonded Geomaterials Subject to Mechanical and/or Chemical Degradation." *International Journal for Numerical and Analytical Methods in Geomechanics* 27(9): 705–32. http://doi.wiley.com/10.1002/nag.294 (September 6, 2012).

Oohashi, Kiyokazu, Takehiro Hirose, Miki Takahashi, and Wataru Tanikawa. 2015. "Dynamic Weakening of Smectite-Bearing Faults at Intermediate Velocities: Implications for Subduction Zone Earthquakes." *Journal of Geophysical Research : Solid Earth* 120: 1572–86.

Proctor, B P et al. 2014. "Dynamic Weakening of Serpentinite Gouges and Bare Surfaces at Seismic Slip Rates." *Journal of Geophysical Research : Solid Earth* 119: 8107–31.

Rattez, Hadrien et al. 2018a. "Numerical Analysis of Strain Localization in Rocks with Thermo-Hydro-Mechanical Couplings Using Cosserat Continuum." *Rock Mechanics and Rock Engineering* 51(10): 3295–3311.

Rattez, Hadrien et al. 2018b. "The Importance of Thermo-Hydro-Mechanical Couplings and Microstructure to Strain Localization in 3D Continua with Application to Seismic Faults . Part II : Numerical Implementation and Post-Bifurcation Analysis." *Journal of the Mechanics and Physics of Solids* 115: 1–29.

Rattez, Hadrien, Ioannis Stefanou, and Jean Sulem. 2018. "The Importance of Thermo-Hydro-Mechanical Couplings and Microstructure to Strain Localization in 3D Continua with Application to Seismic Faults. Part I: Theory and Linear Stability Analysis." *Journal of the Mechanics and Physics of Solids* 115: 54–76.

Rattez, Hadrien, and Manolis Veveakis. 2020. "Weak Phases Production and Heat Generation Control Fault Friction during Seismic Slip." *Nature Communications* 11(350).

Reches, Ze'ev, and David A. Lockner. 2010. "Fault Weakening and Earthquake Instability by Powder Lubrication." *Nature* 467(7314): 452–55. http://www.nature.com/doifinder/10.1038/nature09348.

Rice, James R. 2006. "Heating and Weakening of Faults during Earthquake Slip." *Journal of Geophysical Research: Solid Earth* 111(5).

Scholz, Christopher H. 2002. *The Mechanics of Earthquakes and Faulting*. Second Edi. Cambridge.

Segui, Carolina, Hadrien Rattez, and Manolis Veveakis. 2019. "On the Stability of Deep-Seated Landslides. The Cases of Vaiont (Italy) and Shuping (Three Gorges Dam, China)." *EarthArXiv preprint*.

Spagnuolo, E., S. Nielsen, M. Violay, and Giulio Di Toro. 2016. "An Empirically Based Steady State Friction Law and Implications for Fault Stability." *Geophysical Research Letters* 43(7): 3263–71.

Sulem, Jean, and V Famin. 2009. "Thermal Decomposition of Carbonates in Fault Zones: Slip-Weakening and Temperature-Limiting Effects." *Journal of Geophysical Research* 114(B3): 1–14.

Tembe, Sheryl, David A. Lockner, and Teng Fong Wong. 2010. "Effect of Clay Content and Mineralogy on Frictional Sliding Behavior of Simulated Gouges: Binary and Ternary Mixtures of Quartz, Illite, and Montmorillonite." *Journal of Geophysical Research: Solid Earth* 115(3): 1–22.

Di Toro, Giulio et al. 2011. "Fault Lubrication during Earthquakes." *Nature* 471(7339): 494–98. http://www.nature.com/doifinder/10.1038/nature09838.

Veveakis, E., and K. Regenauer-Lieb. 2015. "Cnoidal Waves in Solids." *Journal of the Mechanics and Physics of Solids* 78(May 2015): 231–48. http://dx.doi.org/10.1016/j.jmps.2015.02.010.

Veveakis, E et al. 2010. "Chemical Reaction Capping of Thermal Instabilities during Shear of Frictional Faults." *Journal of the Mechanics and Physics of Solids* 58(9): 1175–94. http://www.sciencedirect.com/science/article/pii/S0022509610001262 (September 21, 2015).